Laser Light Scattering from Fluctuations Enhanced by Stimulated Raman Scattering

T. Kolber, W. Rozmus, and V. T. Tikhonchuk[a]
Department of Physics, University of Alberta, Edmonton, Alberta, Canada T6G 2J1

Ph. Mounaix and D. Pesme
Centre de Physique Theorique, Ecole Polytechnique, 91128 Palaiseau, CEDEX, France

(Received 5 October 1992)

Numerical analysis of the system of Zakharov and electromagnetic wave equations shows that in the nonlinear stage of saturation of stimulated Raman backscattering a wide spectrum of plasma fluctuations is excited. These fluctuations manifest themselves in enhanced levels of Brillouin and forward Raman scattering. The coupling between stimulated Raman scattering and these secondary scattering processes is theoretically described. We derive new scaling laws for enhanced Brillouin and forward Raman scattering, which can be tested in the current laser-plasma interaction experiments.

PACS numbers: 52.40.Nk, 52.35.Mw, 52.35.Ra

Over the last few years it has become quite evident that to fully understand the behavior of parametric instabilities in laser-produced plasmas one must examine the interactions of the separate processes occurring in the same time frame. A great deal of experimental evidence has been gathered on the interaction of stimulated Raman scattering (SRS) and stimulated Brillouin scattering (SBS) [1–3]. Depending on physical parameters both instabilities can compete for pump energy, and affect each other by disturbing the resonant matching conditions or by enhancing the plasma fluctuation levels [4–7].

In the earlier theoretical studies by Rose, DuBois, and Bezzerides [4] the quenching of SRS by SBS has been described in remarkable agreement with experimental observations [1]. The conclusions of this analysis applied, however, to quite unique plasma conditions corresponding to low temperature and low density CO_2 laser-plasma interaction experiments. The more recent investigations [6, 7] of SBS-SRS nonlinear coupling in long scale short wavelength laser-produced plasmas were limited by the lack of electron-ion collisional damping on Langmuir waves, as well as a proper saturation mechanism for SBS, resulting in unrealistically high levels of SBS reflectivity.

The present study is devoted to the discussion of the consequences of nonlinear SRS saturation on Brillouin and forward Raman scattering. It combines previous results [8] obtained for SRS saturation with a new analysis, which accounts for the laser light scattering from plasma fluctuations produced as the result of SRS nonlinear evolution. In Refs. [7–9] it has been shown that the parametric decay of the SRS driven Langmuir wave produces a wide spectrum of Langmuir and ion acoustic waves. Here we show that these fluctuations can dramatically enhance Brillouin and forward Raman scattering.

In Ref. [8] the system of Zakharov and electromagnetic wave equations (cf. [4, 5]) has been solved with the additional simplification of excluding coupling to SBS. It has been shown that the parametric decay instability (PDI) of the Langmuir waves saturates SRS at the following reflectivity level:

$$R = \frac{8}{27}\gamma_{0R}^2 L^3 \Gamma_{k_A}^A \frac{(k_L v_e)^2 \omega_p}{\omega_0^2 \omega_A v_{g0} v_{gR}^2}. \tag{1}$$

In Eq. (1) $v_e = (T_e/m_e)^{1/2}$, $c_s = (ZT_e/m_i)^{1/2}$, L is the plasma length, and $\Gamma_{k_A}^A$ represents the Landau damping coefficient of the ion acoustic wave (ω_A, k_A) produced during PDI of the SRS driven Langmuir wave (ω_L, k_L); v_{g0} and v_{gR} stand for the group velocities of the pump (ω_0, k_0) and backscattered (ω_R, k_R) waves, respectively. The homogenous SRS growth rate coefficient is given by $\gamma_{0R} = (1/4)v_0 k_L(\omega_p^2/\omega_R\omega_L)^{1/2}$, where v_0 is the electron quiver velocity amplitude in the electric field of the pump wave. The waves participating in SRS interaction satisfy the usual resonant matching conditions $\omega_0 = \omega_L + \omega_R$ and $k_0 = k_L + k_R$. The secondary process of the PDI corresponds to the resonant conditions $\omega_L = \omega_L^{(1)} + \omega_A$ and $k_L = k_L^{(1)} + k_A$, where $(\omega_L^{(1)}, k_L^{(1)})$ characterizes the first component of the Langmuir wave cascade driven by PDI.

The scaling of the SRS reflectivity (1) corresponds to the maximum amplitude E_L of a resonant Langmuir wave according to the expression

$$\frac{E_L}{\sqrt{4\pi n_0^e T_e}} = \left[\frac{32\Gamma_{k_A}^A \gamma_{0R}^2 L}{3\omega_p \omega_A \mid v_{gR} \mid}\right]^{\frac{1}{2}}. \tag{2}$$

E_L (2) can also be represented using the Langmuir wave threshold $E_{\rm th}$ of PDI and the SRS amplification coefficient $A = \gamma_{0R}^2 L/\Gamma_{k_L}^L \mid v_{gR} \mid$, by writing $E_L = E_{\rm th}\sqrt{2A/3}$. The amplification coefficient depends on the linear damping coefficient of Langmuir waves $\Gamma_{k_L}^L$, which describes Landau and collisional damping. Dependence of (2) on the threshold field value $E_{\rm th}$ of PDI leads to interesting experimental consequences, discussed in Ref. [10]. Note that both expressions (1) and (2) do not depend on the damping coefficient $\Gamma_{k_L}^L$ of Langmuir waves. The particular mechanism of Langmuir wave dissipation, for

example, Landau and collisional damping, or increased dissipation due to collapse processes (cf. Ref. [9]), does not directly affect SRS reflectivity but controls the spectrum of plasma waves and hot electron production.

The main features of the one-dimensional Zakharov and electromagnetic wave equations model [8], which lead to Eqs. (1) and (2), can be divided into transient processes and the final saturation regime, which is independent of the initial conditions. During the transient evolution SRS grows at first linearly and saturates due to the onset of PDI. SRS never reaches the linear asymptotic regimes related to absolute or convective instabilities (cf. Ref. [4]) because the nonlinear effects due to PDI occur earlier. The first nonlinear saturation corresponds to a strong flash of backscattered radiation. Next in the transient nonlinear regime we observe development of the PDI cascade and its disruption due to different spatiotemporal evolution of SRS and PDI. In the asymptotic regime the electrostatic fluctuations are characterized by the broad spectra and the SRS reflectivity is well approximated by Eq. (1).

Equation (1) agrees with the simulation results (cf. Ref. [8]) obtained from the Zakharov and electromagnetic wave equations with the additional assumption of excluding the coupling to SBS. This extra simplification limits the validity of R (1) either to the plasma conditions where SBS does not grow in time or SBS does not have time to grow to large levels, as in the cases of short laser pulse duration [11]. In the present study we solve the full system of Zakharov and electromagnetic wave equations [4, 5] including coupling to SBS. We, however, restrict ourselves to the regime where SBS evolution cannot affect the saturation of SRS. Namely, the component of the ponderomotive force responsible for SBS coupling in the equation for ion density is always kept smaller than the component of the ponderomotive force due to SRS produced Langmuir waves, i.e., $8G_B N_{2k_0} k_0 \Gamma^A_{k_A}/k_A\omega_A \ll |E_L|^2/4\pi n_0^e T_e$. Here $G_B = \gamma_{0B}^2 L/v_{g0}\Gamma^A_{2k_0}$ is the SBS gain, γ_{0B} is the homogeneous SBS growth rate, $\Gamma^A_{2k_0}$ is the Landau damping coefficient of the SBS-driven ion waves, and N_{2k_0} denotes the amplitude of the density fluctuation which is responsible for Brillouin scattering. Figure 1 (line 3) shows the above criterion as the upper bound for the region where Brillouin coupling has no effect on SRS saturation. This condition has been evaluated for the amplitude of the SRS-produced Langmuir wave E_L given by the scaling law (2), and for the amplitude of the density fluctuations N_{2k_0} given below by Eq. (4).

We now turn to the analysis of the enhancement of Brillouin and forward Raman scattering resulting from the generation of plasma and ion acoustic waves by the PDI of the SRS-produced plasma wave. From observations of a large number of simulation results we have noticed an exponential decrease towards smaller wave numbers in the Fourier spectra of ion acoustic (N_k) and Langmuir (E_k) waves. In each case illustrated in Fig. 2 the enhanced part of the Langmuir wave spectra can be

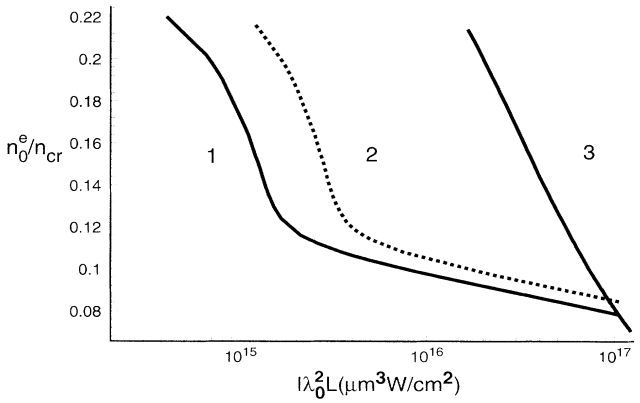

FIG. 1. Parameter space for enhanced Brillouin and forward Raman scattering (for $T_e = 1$ keV): curve 1 corresponds to (5) $2A/3\Delta_B = 1$; curve 2 corresponds to (6) $2A/3\Delta_{FR} = 1$; and curve 3: $G_B(2k_0/k_A)\exp[-c_s \mid k - k_A \mid /\gamma_{PD}] = 1$ is the upper bound of the region, where Brillouin coupling has no effect on the saturation of SRS.

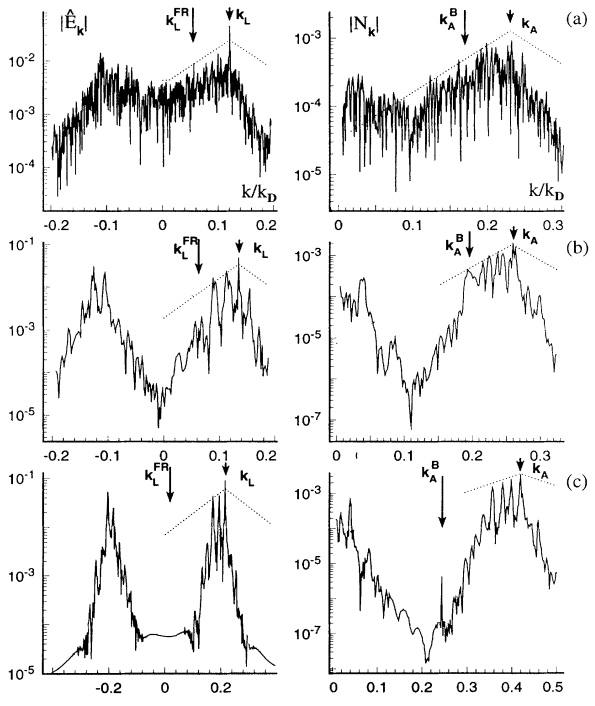

FIG. 2. Fourier spectra of Langmuir ($\hat{E}_k^2 = E_k^2/4\pi n_0^e T_e$) and density ($N_k$) fluctuations: (a) $L = 250$ μm, $I\lambda_0^2 = 2 \times 10^{13}$ Wμm^2/cm^2, $n_0^e/n_{cr} = 0.2$, $T_e = 1$ keV, $ZT_e/T_i = 8$, $Z = 2$; (b) $L = 60$ μm, $I\lambda_0^2 = 5 \times 10^{13}$ Wμm^2/cm^2, $n_0^e/n_{cr} = 0.2$, $T_e = 1.25$ keV, $ZT_e/T_i = 8$, $Z = 5$; (c) $L = 60\,\mu$m, $I\lambda_0^2 = 1 \times 10^{14}$ Wμm^2/cm^2, $n_0^e/n_{cr} = 0.05$, $T_e = 0.4$ keV, $ZT_e/T_i = 6$, $Z = 2$.

approximated by

$$E_k \simeq (E_L/\sqrt{2})\exp[-c_s \mid k - k_L \mid /\gamma_{\rm PD}], \tag{3}$$

where the growth rate of PDI is given by $\gamma_{\rm PD}^2 = \gamma_{\rm PDW}^2 = \omega_p k_A E_L^2/64\pi m_i n_0^i c_s$, in the weakly coupled case ($\gamma_{\rm PD} < k_A c_s$), or by $\gamma_{\rm PD}^3 = (3^{1.5}/4)k_A c_s \gamma_{\rm PDW}^2$, in the strongly driven regime ($\gamma_{\rm PD} > k_A c_s$). The amplitude of the SRS-driven Langmuir wave E_L is calculated from the asymptotic expression (2). Using the approximate relation between plasma waves and ion density fluctuations driven by PDI (cf. Ref. [8]) we can also write for the density spectrum

$$N_k \simeq \frac{1}{8}\frac{\omega_A}{\Gamma_{k_A}^A}\frac{\mid E_L \mid^2}{4\pi n_0^e T_e}\exp\left[-\frac{c_s \mid k - k_A \mid}{\gamma_{\rm PD}}\right]. \tag{4}$$

The discrete components of the PDI cascade, seen very clearly in Figs. 2(b) and 2(c), are separated by $\Delta k = \frac{2}{3}k_D\sqrt{Zm_e/m_i}$ in the Langmuir wave spectrum and by $2\Delta k$ in the density spectrum.

The relevant wave numbers, which will contribute to the enhancement of SBS and forward Raman, are $k_A^B = 2k_0$ and $k_L^{\rm FR} = k_0 - k_R$, respectively. To calculate the enhancement we must know not only the overall shape of the spectra, but also the extent of the enhanced region. It scales as the overall number of steps in the PDI cascade, which is proportional to the ratio $E_L^2/E_{\rm th}^2$ (cf. Ref. [12]). In the case of SRS-driven PDI the averaged number of cascades in the interaction region is $\frac{2}{3}A$ [cf. Eq. (2)]; i.e., it depends directly on the amplification coefficient of SRS (cf. Fig. 2). Using this estimate, we may derive simple strong enhancement criteria in terms of the backward SRS amplification coefficient.

In the case of the Brillouin scattering this criterion is

$$\tfrac{2}{3}A > \mid k_A^B - k_A \mid /2\Delta k = \Delta_B, \tag{5}$$

and for the forward Raman scattering

$$\tfrac{2}{3}A > \mid k_L^{\rm FR} - k_L \mid /\Delta k = \Delta_{\rm FR}. \tag{6}$$

Figure 1 displays the two threshold curves for Eqs. (5) and (6), which define the lower bounds for the parameter space of enhanced scattering. Each panel in Fig. 2 illustrates the different degree to which the strong enhancement criterion is met, i.e., 2(a) $7.1\Delta_B = \frac{2}{3}A$, 2(b) $1.4\Delta_B = \frac{2}{3}A$, and 2(c) $0.4\Delta_B = \frac{2}{3}A$. The runs illustrated in Figs. 2(a) and 2(b) produce strongly enhanced Brillouin reflectivity, while the run of Fig. 2(c) does not display any enhancement above the standard prediction of the three wave coupling theory. According to the criterion (6) forward Raman scattering enhancement was observed in the run corresponding to Fig. 2(a), but not for Fig. 2(b) or 2(c). Note that for the parameters considered in this study one has $\frac{2}{3}A < k_L/\Delta k$ which prevents formation of the Langmuir wave condensate by the PDI cascade.

An example of the time evolution of SRS reflectivity and the very rapid increase in Brillouin and forward Raman scattering are shown in Fig. 3(a). This enhancement occurs relatively early in the nonlinear evolution of PDI, usually after the first maximum in SRS reflectivity at the time when the cascade contains at least two steps and the PDI is extended through a significant part of the SRS interaction region. Comparison of enhanced Brillouin reflectivity with the reflectivity calculated from the standard three wave coupling model in Fig. 3(a) illustrates dramatic enhancement of the Brillouin scattering. Another very distinct property of the Brillouin scattered light is the frequency spectrum shown in Fig. 3(b). One notices redshifted and blueshifted components with respect to the pump frequency. This is a clear indication that this process is quite different from the resonant stimulated Brillouin scattering and takes place on density fluctuations produced by the PDI. The spectrum also shows a well-defined redshifted peak labeled by $\gamma_{\rm PD}^{\rm eff}$. Its shift from the fiducial can be identified with the observed growth rate of PDI.

Scaling expressions for the Brillouin and forward Raman reflectivities can now be calculated from the equations for the enhanced fluctuations of E_k (3) and N_k (4). Following standard arguments of three wave coupling (cf. Ref. [8]) and neglecting pump depletion we have obtained

$$R_B = [\alpha_B \mid N_{2k_0} \mid L]^2 \tag{7}$$

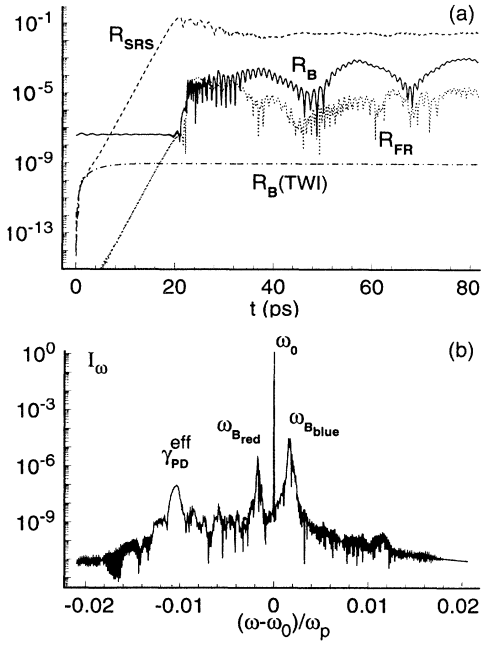

FIG. 3. Result of simulations for parameters of Fig. 2(b): (a) Time evolution of stimulated Raman scattering $R_{\rm SRS}$, enhanced Brillouin $R_{\rm B}$, and forward Raman $R_{\rm FR}$, as well as Brillouin reflectivity for the standard three wave interaction model $R_{\rm B}$(TWI). (b) Frequency spectrum of pump and Brillouin backscatter at the left boundary ($x = 0$).

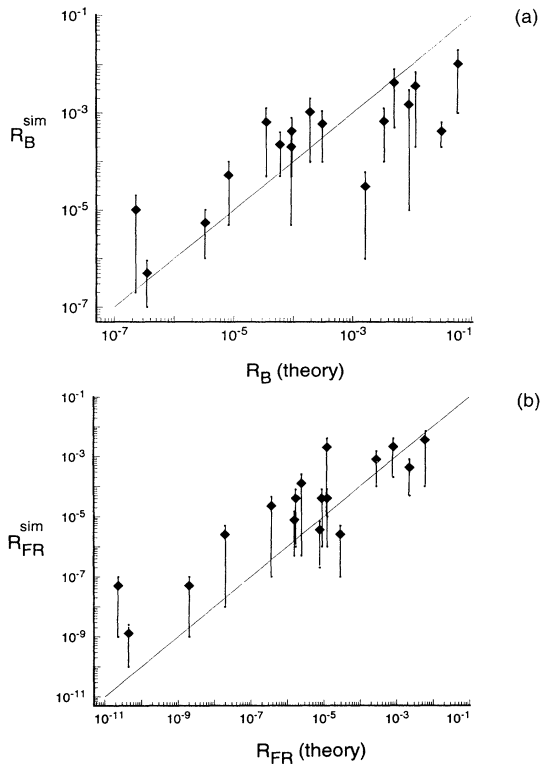

FIG. 4. Simulation reflectivities vs theoretical predictions for (a) enhanced Brillouin scattering Eq. (7), and (b) enhanced forward Raman scattering Eq. (8). All runs are for parameters corresponding to the region of enhanced scattering defined by Fig. (1).

and

$$R_{\rm FR} = \left[\alpha_{\rm FR} \mid E_{k_L^{\rm FR}} \mid L\right]^2 \tag{8}$$

where $\alpha_B = \omega_p^2/2\omega_0 v_{g0}$ and $\alpha_{\rm FR} = k_L^{\rm FR} e/4m_e\omega_0\sqrt{v_{g0}v_{gR}}$ are the coupling coefficients for the Brillouin and forward Raman scattering processes. The scaling laws (7) and (8) have been compared with simulation data.

Results of these comparisons are displayed in Fig. 4, where the physical parameters of the simulations have been chosen from the region defined in Fig. 1. Vertical error bars define minimum and maximum values in time and the diamonds represent the time averaged data of reflectivity. Experimental testing of these scaling laws may provide efficient tools for diagnostics and control of laser light scattering processes in a plasma corona of inertial confinement fusion targets. These expressions display very strong dependence of the reflectivities on the interaction length L in a plasma. In our simulations L was a free parameter because we explored the model of a homogeneous plasma slab. But in practice L depends on the plasma inhomogeneity length, laser beam focusing conditions, and plasma wave damping. Our simulations show that decreasing the interaction length may have dramatic effects on all scattering processes in the plasma.

In summary, we have discussed the effect of the nonlinear SRS saturation on the secondary scattering processes. The nonlinear evolution of the parametric decay of SRS-driven Langmuir waves results in broad fluctuation spectra, which enhance Brillouin and forward Raman scattering. Brillouin scattered light is characterized by comparable blueshifted and redshifted components in the frequency spectrum. Analytical expressions for the shape of the turbulent spectrum of Langmuir and ion acoustic waves have been proposed. Finally the region of enhancement and scaling laws for the reflection coefficients have been determined. Our results are independent from initial noise levels and could be easily tested in experiments.

The authors acknowledge many useful discussions with Don DuBois, Harvey Rose, and Bandel Bezzerides. We also appreciate several conversations with Hector Baldis, Paul Drake, and Christine Labaune. Many thanks go to John Samson and the Canadian Network for Space Research for providing the computers used for our simulations. This work was partially supported by the Natural Sciences and Engineering Research Council of Canada.

[a] On leave from the P. N. Lebedev Physics Institute, Russian Academy of Science, Moscow, Russia.

[1] C. J. Walsh, D. M. Villeneuve, and H. A. Baldis, Phys. Rev. Lett. **53**, 1445 (1984); D. M. Villeneuve, H. A. Baldis, and J. E. Bernard, Phys. Rev. Lett. **59**, 1585 (1987).

[2] H. A. Baldis, P. E. Young, R. P. Drake, W. L. Kruer, K. Estabrook, E. A. Williams, and T. W. Johnston, Phys. Rev. Lett. **62**, 2829 (1989).

[3] H. A. Baldis, D. M. Villeneuve, C. Labaune, D. Pesme, W. Rozmus, W. L. Kruer, and P. E. Young, Phys. Fluids B **3**, 2341 (1991).

[4] H. A. Rose, D. F. DuBois, and B. Bezzerides, Phys. Rev. Lett. **58**, 2547 (1987).

[5] W. Rozmus, R. P. Sharma, J. C. Samson, and W. Tighe, Phys. Fluids **30**, 2181 (1987).

[6] K. Estabrook, W. L. Kruer, and M.G.Haines, Phys. Fluids B **1**, 1282 (1989).

[7] G. Bonnaud, D. Pesme, and R. Pellat, Phys. Fluids B **2**, 1618 (1990).

[8] T. Kolber, W. Rozmus, and V. T. Tikhonchuk, Phys. Fluids B **5**, 138 (1993).

[9] B. Bezzerides, D. F. DuBois, and H. A. Rose (to be published).

[10] R. P. Drake and S. H. Batha, Phys. Fluids B **3**, 2936 (1991).

[11] H. A. Baldis, H. C. Barr, D. M. Villeneuve, G. D. Enright, C. Labaune, and S. Baton, Proc. SPIE Int. Soc. Opt. Eng. **1229**, 144 (1990).

[12] W. L. Kruer and E. J. Valeo, Phys. Fluids **16**, 675 (1973); V. P. Silin and V. T. Tikhonchuk, Phys. Rep. **135**, 1 (1986).